Electronic Supplementary Material (ESI) for Journal of Materials Chemistry A.

Supporting Information

Promoted high temperature carrier mobility and thermoelectric performance of InTe enabled by altering scattering mechanism

Huaxing Zhu,[a] Bin Zhang,[b] Guiwen Wang,[b] Kunling Peng,[a] Yanci Yan,[a] Qing Zhang,[c] Xiaodong Han,[c] Guoyu Wang,[d] Xu Lu,[*a] and Xiaoyuan Zhou[*ab]

[a] *Chongqing Key Laboratory of Soft Condensed Matter Physics and Smart Materials, College of Physics, Chongqing University, Chongqing 401331, P. R. China*
[b] *Analytical and Testing Center of Chongqing University, Chongqing 401331, P. R. China*
[c] *Beijing Key Laboratory and Institute of Microstructure and Property of Advanced Materials, Beijing University of Technology, Beijing 100124, P. R. China*
[d] *Chongqing Institute of Green and Intelligent Technology, Chinese Academy of Sciences, Chongqing 400714, China*

Contact Authors: luxu@cqu.edu.cn; xiaoyuan2013@cqu.edu.cn

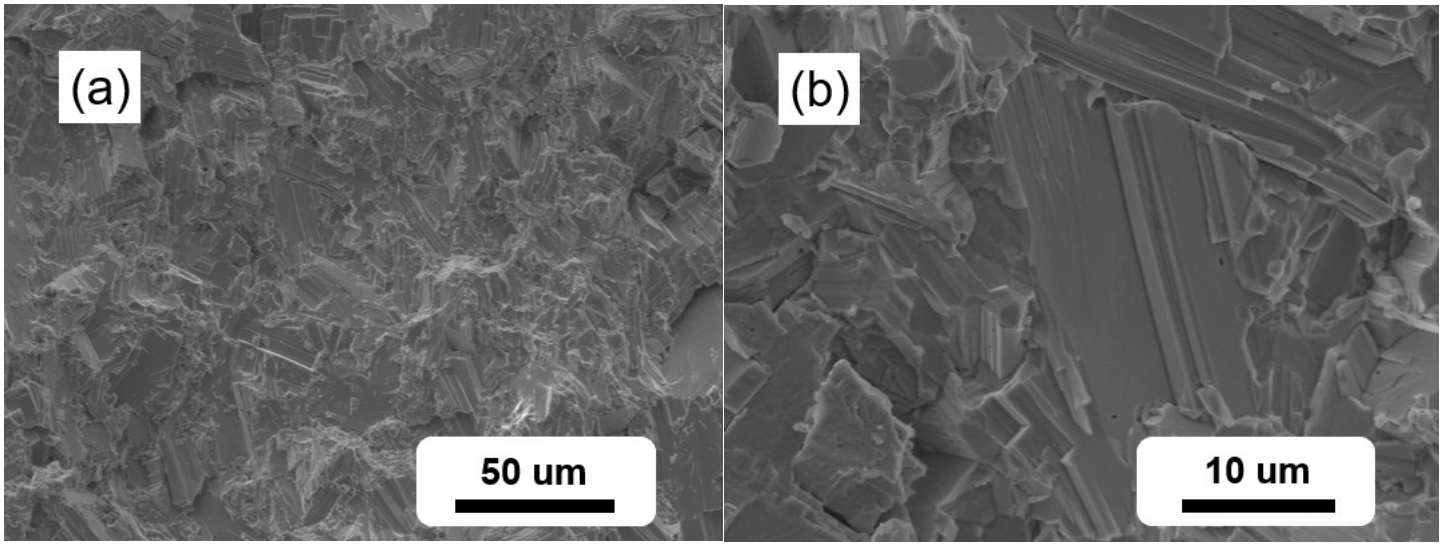

Figure S1. The typical SEM images[S1] of pristine InTe: (a) reveals a dense structure with a well-organized morphology composed of plate-like crystallites and the average grain size at the surface is around 15 um, (b) clearly shows the layered structure in an enlarged area of the grains.

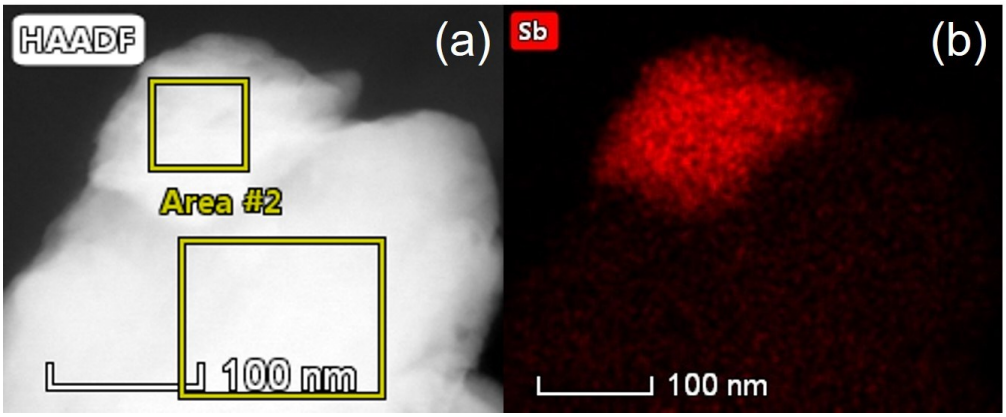

Figure S2. (a) HAADF image in an enlarged area in Fig. 2(a) and (b) an overlay of Sb's mapping on the HAADF image.

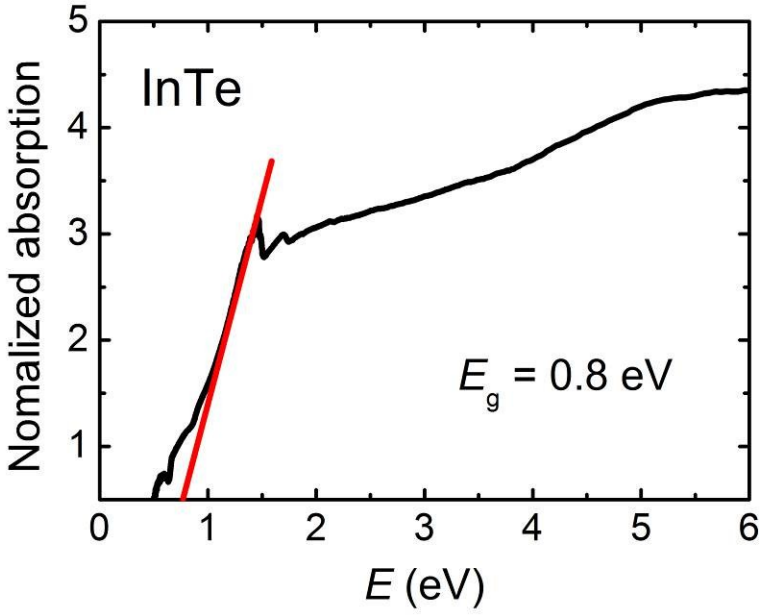

Figure S3. An optical band gap[S2] of about 0.8 eV is estimated for pristine InTe.

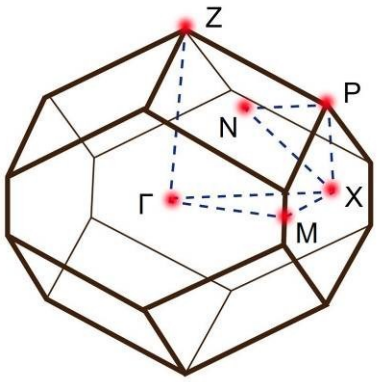

Figure S4. The high symmetry points served to calculate electronic structure and lattice dynamics for InTe in the Brillouin zone.

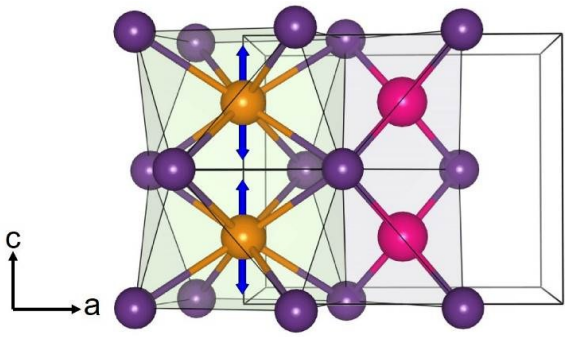

Figure S5. Schematic of localized vibrational modes in pristine InTe mainly originating from In^{+} cations (orange spheres). It is proposed that the lowest frequency Einstein oscillators (Θ_{E1} = 30.2 K/ 2.6 meV) is associated with the motion of the In+ cations along c direction.

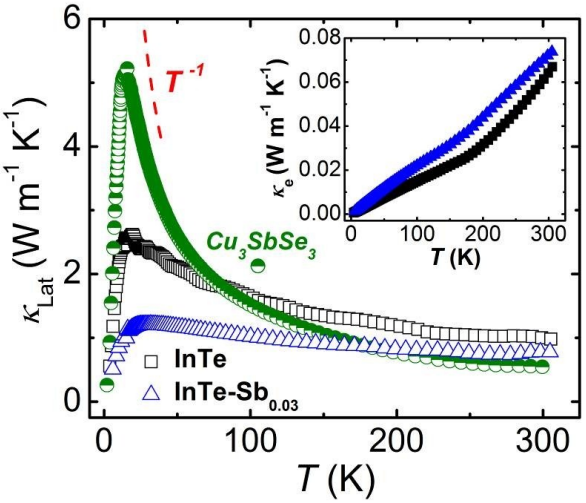

Figure S6. Measured low-temperature lattice thermal conductivity κ_{Lat} of InTe and InTe-$Sb_{0.03}$, inset shows the negligible contribution from κ_e. We have observed pronounced dielectric peak around 19 K which means our samples can still be considered crystalline.[S3] Both of the two samples exhibit κ_{Lat} value around 1 W m^{-1} K^{-1} near room temperature, and are comparable to the well-known Cu_3SbSe_3 compound (green line)[S4] with ultralow κ_{Lat} in the whole temperature range.

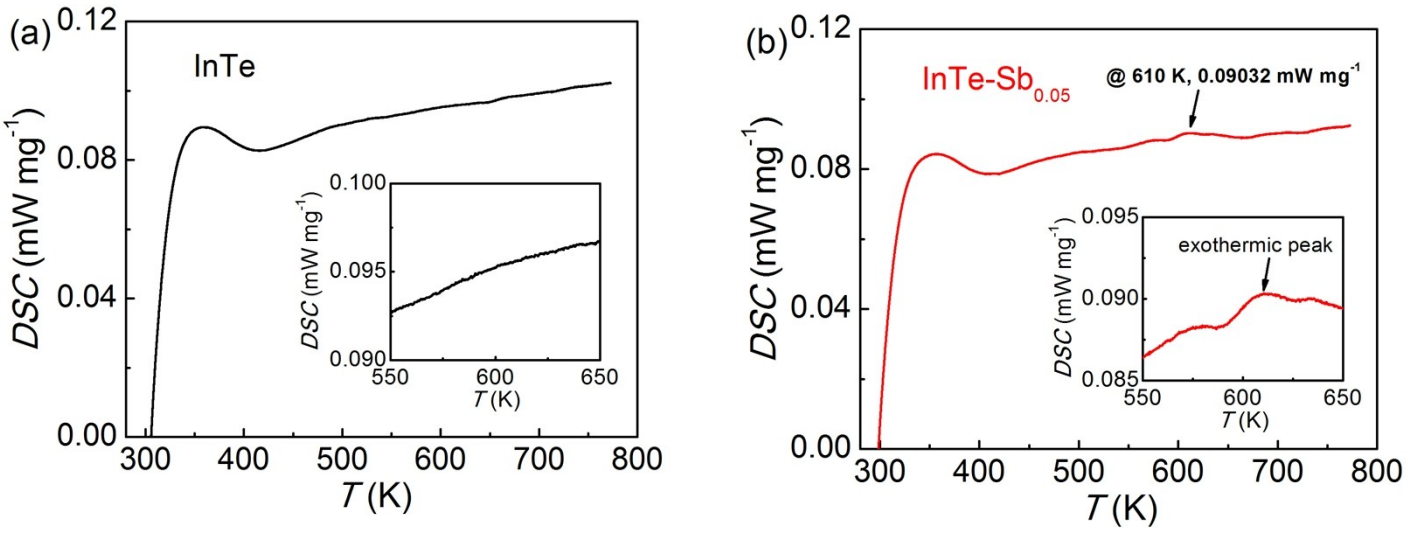

Figure S7. DSC results for (a) InTe and (b) InTe-$Sb_{0.05}$. A weak exothermic peak is observed around 610 K in InTe-$Sb_{0.05}$ sample.

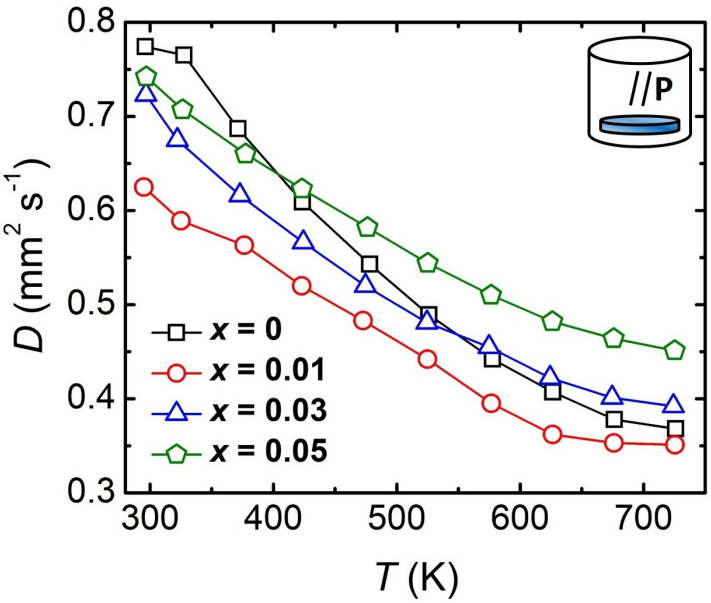

Figure S8. Temperature-dependent thermal diffusivity of InTe and InTe-Sb_x (x = 0.01, 0.03, 0.05) samples. The thermal diffusivity is measured along the same direction as that for electrical transport measurement, parallel to the pressing direction.

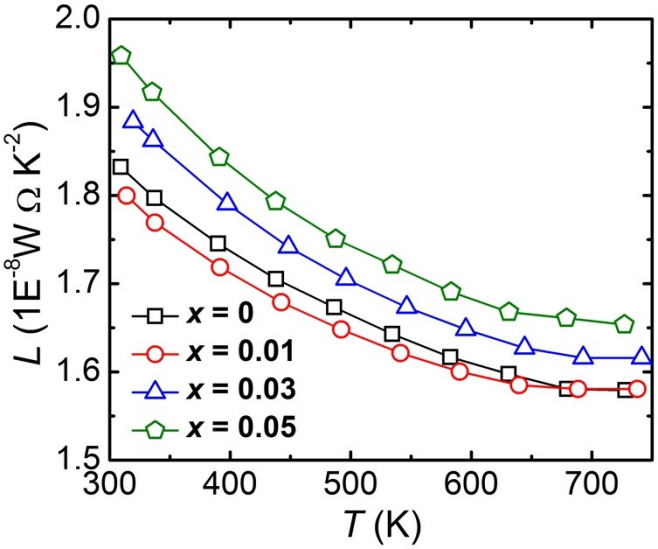

Figure S9. Temperature-dependent Lorenz numbers of InTe and InTe-Sb_x (x = 0.01, 0.03, 0.05) samples. The Lorenz numbers are deduced from the Seebeck coefficient and based on SPB model.[S5]

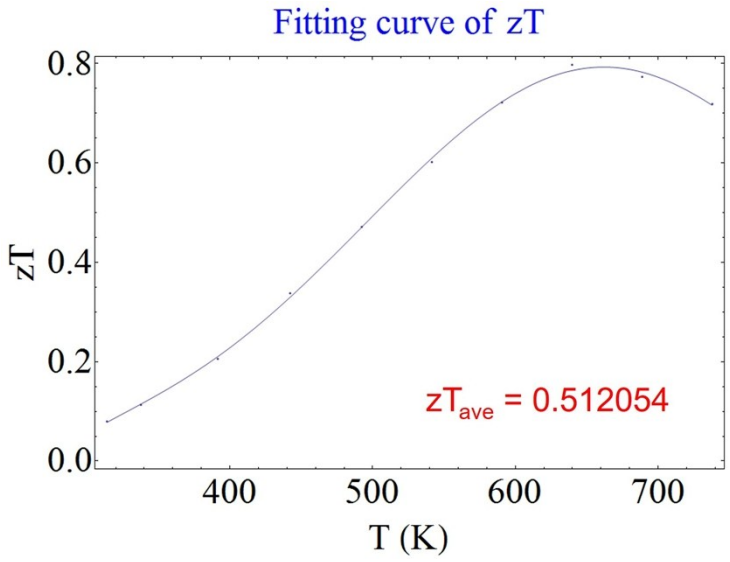

Figure S10. The calculated average *zT* for InTe-$Sb_{0.01}$. The fitting curve is fitted from the data of *zT* values according to the below equation:

$$zT(T) = \sum_{i=0}^{5} C_i T^i \qquad \text{(S1)}$$

where *T* the absolute temperature and C_i the fitting constants for each power of *T*.

The zT_{ave} is calculated by:

$$zT_{ave} = \frac{\int_{T_{min}}^{T_{max}} zT(T)\,dT}{T_{max} - T_{min}} \qquad \text{(S2)}$$

where T_{min} and T_{max} are the minimum and maximum temperature, respectively in the required temperature range.

Table S1. Atom parameters of InTe in tetragonal phase. Calculated unit cell formula weight: 1939.360; density: 6.318 g cm^{-3}. Rp = 0.0323; wRp = 0.0416.

Atom parameters for phase no. 1							
			frac	x	y	z	100*Uiso
In	+1	Values:	1.000	0.000000	0.000000	0.250000	4.007
		Sigmas:					0.083
		Shft/esd:					-0.01
In	+3	Values:	1.000	0.000000	0.500000	0.250000	0.265
		Sigmas:					0.060
		Shft/esd:					-0.04
Te	-2	Values:	1.000	0.182627	0.682626	0.000000	-0.164
		Sigmas:		0.000091	0.000091		0.032
		Shft/esd:		0.01	0.01		-0.07
Maximum atom shift: 0.00							
Atomic parameter sum (shift/ error)*2 for phase 1: 0.01							

Table S2. The coordinates of symmetry k-points.

	$\times\mathbf{b}_1$	$\times\mathbf{b}_2$	$\times\mathbf{b}_3$
Γ	0	0	0
M	-1/2	1/2	1/2
N	0	1/2	0
P	1/4	1/4	1/4
X	0	0	1/2
Z	*η*	*η*	*-η*
$\eta = (1+c^2/a^2)/4$			

Table S3. Fitting parameters for modelling *C*p vs. *T* plot.

Parameter	InTe		InTe-$Sb_{0.03}$	
$\gamma/10^{-3}$ J mol^{-1} K^{-2}	/		/	
Θ_{E1}/ K	30.2 ± 2.7 K	α_{E1} = 0.009	40.3 ± 3.0 K	α_{E1} = 0.045
Θ_{E2}/ K	55.7 ± 3.2 K	α_{E2} = 0.108	60.2 ± 3.5 K	α_{E2} = 0.117
Θ_{E3}/ K	76.5 ± 5.1 K	α_{E3} = 0.318	97.5 ± 5.4 K	α_{E3} = 0.314
Θ_D/ K	200 K	α_D = 0.57	200 K	α_D = 0.57

Table S4. Through fitting the κ_{Lat} of pristine InTe, we obtain the pre-factor *B* of Umklapp scattering relaxation time. The detailed calculation of point defects scattering can be found elsewhere.[S6] A sound velocity ~1570 m/s reported by Jana et al. is used for the fitting process and the Debye temperature value ~200 K is estimated from the Low-temperature *C*p in our study. B_H is a high order four-phonon scattering coefficient.

Scattering type	**Parameter**	**Value**
Umklapp scattering	B (10^{-17} s/K)	4.4
Point defects scattering	Γ_{expt}	0.0233
	A (10^{-41} s^3)	1.5
	Sound velocity v_s (m/s)	1570
	Debye temperature Θ_D (K)	200
Four-phonon scattering	B_H (10^{-21} s/K^2)	3.0

Supplementary References

S1. X. Liu, T. Li, X. Q. Zhao, H. Suo, Z. Y. Zhang, P. J. Zhao, S. Gao and M. Niu, *Dalton Trans.,* 2018, **47**, 6713.

S2. B. Q. Zhou, S. Li, W. Li, J. Li, X. Y. Zhang, S. Q. Lin, Z. W. Chen and Y. Z. Pei, *Acs Appl. Mater. Interfaces,* 2017, **9**, 34033.

S3. S. Wang, S. Hui, K. L. Peng, T. P. Bailey, W. Liu, Y. G. Yan, X. Y. Zhou, X. F. Tang and C. Uher, *Appl. Phys. Lett.,* 2018, **112**, 142102.

S4. E. J. Skoug and D. T. Morelli, *Phys. Rev. Lett.,* 2011, **107**, 235901.

S5. Y. C. Yan, H. Wu, G. Y. Wang, X. Lu and X. Y. Zhou, *Energy Storage Mater.,* 2018, **13**, 127.

S6. A. Petersen, S. Bhattacharya, T. M. Tritt and S. J. Poon, *J. Appl. Phys.,* 2015, **117**, 035706.